Flux-Velocity Relation for H_2 Outflows [1]

Luis Salas[2] and Irene Cruz-González[3]

ABSTRACT

We present an analysis of velocity resolved near-IR molecular hydrogen observations of a variety of protostellar outflows with very different energetics, degrees of collimation and morphologies. Observations in the 2.12 μm line of H_2 were obtained using an IR Fabry-Pérot interferometer with a spectral resolution of 23 km s^{-1}. The integrated flux-velocity diagrams for each outflow show a flat spectrum for low velocities followed by a decreasing power law $dF/dv \propto v^{\gamma}$, with γ between -1.8 and -2.6, for velocities higher than a clearly defined break velocity at 2 to 17 km s^{-1}. Contrary to shock model predictions it is shown that the H_2 intensity is constant with velocity. We argue that the flux-velocity relation can then be interpreted as a mass-velocity relation, in striking similarity to the power law mass spectra observed in CO outflows. By comparing H_2 and CO mass-velocity spectra, it is shown that there is a velocity regime where both molecules coexist and produce similar γ values. Evolution effects in outflows show as a correlation between outflow length and γ, as outflows age the spectra becomes steeper. Our results support a common physical origin for both CO and H_2 emission and a strong association between the molecular outflows traced in each molecule.

Subject headings: Stars: formation – ISM: kinematics and dynamics – ISM: jets and outflows – ISM: molecules

1. Introduction

Molecular outflows observed in CO show a mass-velocity (MV) relation in the form of a power law $dm(v)/dv \propto v^{\gamma}$ (Rodríguez et al. 1982; Masson & Chernin 1992; Lada & Fich 1996; Davis et al. 1998; Shepherd et al. 1998; Yu, Billawala & Bally 1999) with an index γ ranging from -1.3 to -4. Theoretical models of molecular outflows seek to explain this relationship (Cabrit, Raga & Gueth 1997). So do the numerical models of jet and wind driven outflows (Smith, Suttner & Yorke 1997; Zhang & Zheng 1997; Downes & Ray 1999; Lee et al. 2000; Downes & Cabrit 2001), as well as analytical models of x-wind driven outflows (Matzner & McKee 1999). The MV power law is also obtained as a general property of entrained turbulent flows (Stahler 1994).

Breaks in the MV power law have been observed in some outflows, with a shallower index ~-2 for low velocities (v < 15 km s^{-1}) and steeper, even as low as -8 (Shepherd et al. 1998), for high velocities (v > 30 km s^{-1}). It has also been noted that in some cases γ steepens for older or more energetic outflows (Davis et al. 1998; Shepherd et al. 1998). This behavior may be explained by older outflows developing reservoirs of slowly moving material (Smith, Suttner & Yorke 1997). The viewing angle also affects the observed value of γ. According to numerical models (Smith, Suttner & Yorke 1997; Downes & Cabrit 2001), γ steepens and break velocities decrease as the outflow is viewed closer to the plane of the sky.

The relationship between molecular outflows traced in CO and H_2 is not yet clear. It is believed that H_2 emission associated with outflows originates in shock excited regions, where the out-

[1] Based on observations obtained at the Observatorio Astronómico Nacional at San Pedro Mártir, B.C., México.

[2] Observatorio Astronómico Nacional, IA-UNAM. Apdo. Postal 877, Ensenada, B.C. 22830, México. salas@astrosen.unam.mx

[3] Instituto de Astronomía, UNAM. Apdo. Postal 70-264, C.U., México, D.F. 04510, México. irene@astroscu.unam.mx

flow interacts with its surroundings or with parts of itself moving at different velocities. In this respect, there is evidence of its association with other shock tracers, as is the case of some optical HH objects. However, the very high velocities (>100 km s^{-1}) usually inferred from such interactions impose an additional problem for the survival of the H_2 molecules. On the other hand, the CO molecule does not require such an extreme regime to be excited and it is usually associated with cool gas within the outflow.

In this paper, we present the discovery of a flux-velocity relation for H_2 outflows similar to the CO mass-velocity relation, which is found in outflows with different morphologies, degrees of collimation and energetics.

2. Central velocity observations

As part of an ongoing survey of the kinematics of H_2 outflows, we have carried out observations of the 2.12 μm line of H_2, using a cooled scanning Fabry-Pérot etalon with R=15000. The instrumental setup is described in Salas et al. (1999). Observations were acquired during 1997 and 1998 with the IR camera/spectrograph CAMILA (Cruz-González et al. 1994) at the 2.12 m telescope at the Observatorio Astronómico Nacional (UNAM) in San Pedro Mártir, B.C. (Mexico). Objects with very different energetics, collimation degrees and morphologies were selected including OMC-1 (Salas et al. 1999), HH 211 (Salas, Cruz-González & Rosado 2001), Ceph A (Salas et al. 2001), DR 21 (Cruz-González, Salas & Porras 2001), HH 212 (consistent with the results presented by Davis et al. 2000) and S187IR (Salas, Cruz-González & Porras 1998; Salas, Cruz-González & Rosado 2000).

For each outflow we obtain 26 velocity maps at 9.8 km s^{-1} intervals, for an instrumental FWHM of 23±1 km s^{-1}. In these maps, molecular hydrogen emission is identified and validated on a pixel by pixel basis. For each pixel we identify the velocity channel where the maximum intensity appears, checking that it is not an isolated spike and that the signal level is at least 5σ above the continuum for that particular pixel. After that, a centroid velocity is calculated from 5 channels surrounding the maximum. We further eliminate spurious isolated pixels by requiring each pixel to be contiguous to at least two other pixels with significant emission. This procedure allow us to select pixels with sufficient signal-to-noise forming parts of coherent structures. Analyzing the velocity centroid dispersion in such adjacent pixels, we estimate an intrinsic uncertainty in the velocity measurements of no more than 3 km s^{-1}.

3. Flux-velocity relation

In order to construct a flux - velocity (FV) diagram, the intensity and velocity for every validated pixel in the images is ordered in bins of velocity $|v_{obs} - v_{rest}|$, with respect to the rest velocity of the region obtained from data in the literature. The fluxes are calculated by adding up all the intensities of pixels within each velocity bin along the extent of the outflow, as is usually done with millimeter CO data. This procedure has the disadvantage of loosing spatial information, but in return it greatly increases the signal to noise, particularly at the high velocity end where the data is sparser. After adding up binned data, we divide the obtained flux by the width of the velocity bin to obtain dF/dv.

In Fig. 1 we present the FV diagrams for the outflows in our sample. We have chosen bins of equal logarithmic width of 0.1 dex for all outflows. This width is a compromise between the need to have at least three pixels per bin and the possibility of recovering some high frequency structure in the diagrams. The number of pixels in each velocity bin varies according to the extent and luminosity of each outflow. In the case of OMC-1 there are ~40 pixels per bin, while in HH 211 only 5 and 4 in S 187IR. Bins with less than 3 pixels are not shown in the FV diagram, nor used in the analysis due to lower statistical significance. The error bars in each point are approximately the size of the point markers, but can go up to 3 times higher in some outflows like HH 212.

The FV spectra of all the H_2 outflows presented in Fig. 1 show a similar behavior. Spectra are flat for low velocities and, after a break, decrease as power laws $dF/dv \propto v^{\gamma}$. The power law slopes γ range from -1.8 to -2.6 and the break velocities (v_{break}) are found between 2 and 17 km s^{-1}. Table 1 lists best fit γ and v_{break} values for the outflows in our sample. There is a loose correlation (r = 0.8) between γ and v_{break}, in the sense that objects with steeper γ tend to have higher v_{break}. This relation, would then indicate that FV slopes, as well as break velocities, are different for each outflow.

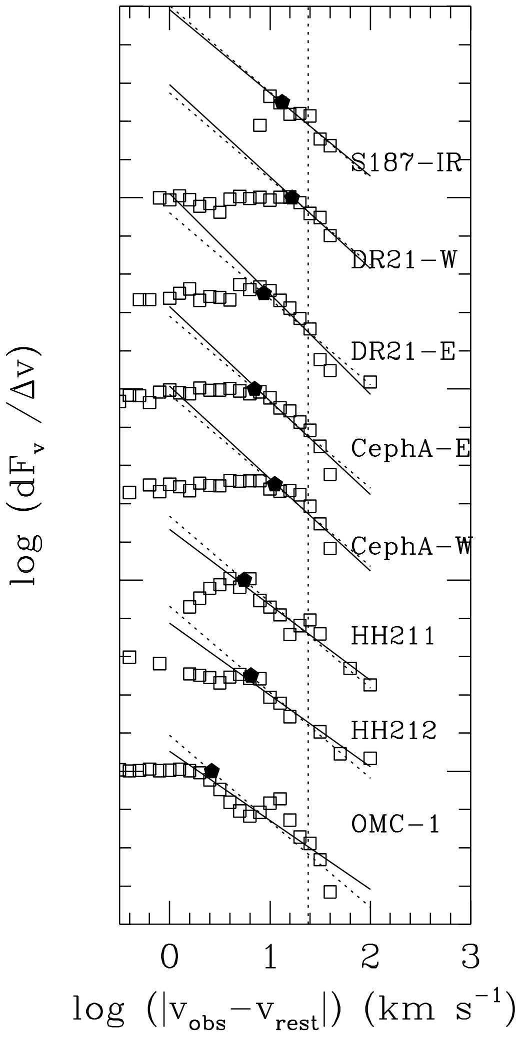

Fig. 1.— Flux velocity spectra for H_2 outflows: S187 IR, DR21 W and E, CephA E and W, HH 211, HH 212, OMC-1. The vertical dotted line shows $v = 24$ km s^{-1}. Fits for a power law with the best fit γ (solid line) and the global mean γ=-2.25 (dotted lines) are shown. The black dot marks the position of the break velocity.

The FV power law is maintained up to about 40 km s^{-1}. In the high velocity end, spectra show different trends; in some cases there is a steeper (Ceph A) or shallower (DR 21E, HH 212) change of slope, while in others no emission is detected (S187IR, DR 21W). HH 211 and OMC-1 are special cases in which a second bump is observed.

Although the differences in v_{break} seem to be real, they could arise if a similar velocity is affected by different viewing angles, rather than being due to an intrinsic difference of the outflows. Objects with low v_{break} values, as HH 211 and HH 212, are known to lie near to the plane of the sky (small φ). However, according to numerical models (Smith, Suttner & Yorke 1997, Downes & Cabrit 2001), a smaller φ results in steeper mass indexes γ and smaller v_{break} (in models that show breaks). Even if we do observe lower v_{break} for outflows known to lie near the plane of the sky, the corresponding values of γ are shallower, not steeper. In fact, we have pointed out a correlation between γ and v_{break} in this sense. This result suggests that inclination is not as important as some other underlying process to drive the values of v_{break} and γ. A fully turbulent outflow, where emitting eddies move in random directions at speeds comparable to the outflow velocity, would be a way in which the importance of φ could be attenuated. In the case of turbulence, v_{break} might be related to the Alfven speed v_A. A shock velocity of $5v_A$ marks the transition between stable and unstable C-shocks (Wardle 1990), and this could in turn relate the observed flux velocity relation to the onset of magnetic turbulence.

A similar relation to the FV is also obtained for the solid angle Ω as a function of velocity, by counting pixels (units of solid angle) within each velocity bin. This result is consistent with the assertion that on the average, the H_2 intensity is not a function of velocity. This result is shown in Fig. 2, where the intensity or surface brightness ($dF_\nu/d\Omega$) is shown to be constant with velocity.

An important implication of this result, is that the FV relation can then be interpreted as a mass-velocity relation, adding to the similarities with

Table 1
Power law index and break velocity

Object	γ	v_{break}
HH211	2.0 ± 0.2	5.5
HH212	1.9 ± 0.1	6.5
OMC-1	1.8 ± 0.3	2.6
CephA-W	2.4 ± 0.5	11.2
CephA-E	2.5 ± 0.3	7.0
DR21-E	2.6 ± 0.3	8.7
DR21-W	2.2 ± 1.0	16.6
S187IR	2.2 ± 0.4	13.2

CO outflows.

Furthermore, if the observed velocity were determined by the shock velocity then, contrary to the observations, one would expect a strong dependence of the intensity on the velocity (of the kind $I \propto v^{\alpha}$), allowing for differences in inclination angle and density of the medium. Depending on the type of shock involved, α should take values of 0 if reformation behind a fast J-shock is allowed (Hollenback & McKee 1989), 1.7 for pure J-shocks (Kwan 1977) and between 4 to 10 for C-shocks (Draine et al. 1983) depending greatly on the geometry involved (Fernandes et al. 1997). High values of α are definitely excluded from our results, while the large velocities involved in the fast J-shocks of Hollenback & McKee (1989) are beyond the interval of velocities considered here. And yet, many of these shock types have been identified in molecular outflows. It is then clear that the observed velocity cannot be dominated by the shock velocity alone. This result is consistent with hydrodynamical simulations of jets propagating into a surrounding molecular medium (e.g. Raga et al. 1995; Suttner et al. 1997) where low velocity line profiles are dominated by emission from the non-dissociative oblique shocks arising at the sides of the bow shocks.

We conclude that all outflows detected in H_2 have similar power law behaviors in flux vs. velocity, solid angle vs. velocity and mass vs. velocity.

4. Mass velocity relations

The behavior of the mass velocity spectrum of CO and H_2 outflows is shown schematically in Fig. 3. CO outflows show a power law from low velocities up to a break point, $v_{break}(CO)$, where in some sources a steepening is observed in the high velocity regime. H_2 outflows show a flat spectrum and a break ($v_{break}(H_2)$) at low velocities, beyond which it also behaves as a power law. Both observed breaks define three different velocity regimes. The regime between $v_{break}(H_2)$ and $v_{break}(CO)$ shows a similar power law for both molecules, and may arise from shocked regions in the outflow where both molecules coexist and contribute to the cooling, perhaps only differentiated by being in different temperature regions along the cooling zones of the shocks. In the regime below $v_{break}(H_2)$, although a the flattening of the H_2 slope is observed, the emission may also arise from shocked regions along the outflow. A corresponding flattening of the CO spectrum has not been reported, possibly due to the confusion with the emission from the quiescent molecular cloud. It is also possible that the CO power law extends to lower velocities, dominated by cool material that is swept by the outflow. That material may excite the emission from the CO molecules (in J=1-0 and 2-1) but not that from H_2. At higher velocities ($v > v_{break}(CO)$), no H_2 emission is observed, probably due to the dissociation of the H_2 molecules.

Numerical models of molecular outflows are able to reproduce the mass velocity relation observed in CO. In the simulations done by Smith et

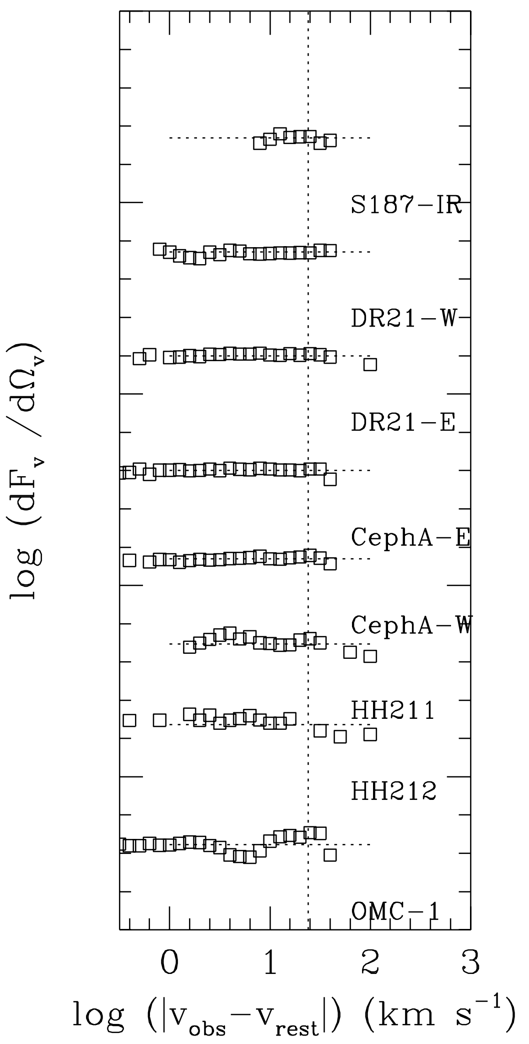

Fig. 2.— Plot of intensity vs. velocity shows no velocity dependence. The vertical dotted line corresponds to $v = 24$ km s^{-1}.

al. 1997, a power law is observed from low to high velocities. However these simulations do not have a grid small enough to resolve the shocked regions. Downes and Ray (1999), use higher resolution to better resolve the cooling zones, and a flattening of the slope is appreciable for low speeds. However the lowest velocities ($v < 10$ km s^{-1}) are not examined in their analysis. Downes and Cabrit (2001) examine even lower velocities, and still a shallower slope is found, consistent with the flat slope observed in H_2. At the high velocity end, these authors find a steepening of the MV spectrum, consistent with the observed increase of the slope for CO outflows, followed by a bump at the projected velocity of the bow apex. In this region it is predicted that the H_2 molecule will dissociate, and no emission is observed.

5. Comparison between outflow parameters

It is known that the mass-velocity index for CO outflows is related with outflow parameters such as the mass loss rate and dynamical age of the outflow (Richer et al. 2000; Yu, Billawala & Bally 1999), in the sense that γ steepens for more energetic or older outflows (Davis et al. 1998). In the case of H_2 outflows we also note these trends. A correlation between the outflow length and either v_{break} or γ is discussed.

In CO outflows it has been argued that the energetics or luminosity of the source may be related to γ (Davis et al. 1998). Evolution effects have also been posed as a possible cause for the steepening of γ in outflows (Smith, Suttner and Yorke 1997).

For H_2 outflows, we compare the mass loss rate $\dot{M}_w$ obtained from data in the literature with γ and v_{break}. The correlation we find is poor, influenced by the cases of OMC-1 and S187IR. OMC-1 has a large $\dot{M}_w$ for low γ and v_{break} values, while S187IR shows the contrary. It seems that the dynamics of H_2 gas is not necessarily driven by the mass loss rate alone, which spans a range of four orders of magnitude for the objects in the sample. As is shown by Richer et al. (2000), for CO outflows, the mass spectrum shows no evidence of correlation with the source bolometric luminosity. That is, the energetics of the flow ($\dot{M}_w$ and L_{bol}) and γ may not be exclusively related. They also argue that probably γ decreases with the dynamical age of the outflow.

To study the evolution effects, we first compare two directly measurable quantities, the break velocity and the length of the outflow (l) measured from the driving source position. Fig. 4 shows a correlation ($r = 0.85$) for the relation $v_{break} \propto l^{0.4}$. Similarly, $|\gamma| \propto l^{0.08}$ with r=0.82. If the expansion velocities of the outflows are similar, this correlation implies an age vs. γ relation. In fact, steeper γ and larger v_{break} are found in older outflows in our sample (DR21: 10^4; CephA) while younger outflows (HH 211: 300 y;, OMC-1: 1000 y) show shallower γ and smaller v_{break}.

CO outflows show a break velocity in the high-velocity end. It is observed that the youngest CO flows have the largest range of velocities and highest break velocities, while older flows have smaller ranges and break velocities (Yu, Billawala & Bally 1999). As outflows age, these authors propose that the break velocity may decrease to the point at which the shallow part of the CO mass spectrum slope is hidden within the ambient cloud line core, leaving only the steep slope component to be observed. The H_2 outflows show a break at low velocities, and we note that low v_{break} values correspond to younger sources while larger v_{break} values correspond to older sources and in both cases the observed velocity range is similar. This posses an evolution scenario where the break velocity observed in H_2 appears at low velocity and increases with age, while that observed in CO appears at high velocity and then decreases. As outflows age, the reservoir of shocked H_2 gas would produce a flat mass spectrum over a wide velocity range. Numerical models of evolved outflows are needed to test this result.

6. Conclusions

The H_2 kinematics of outflows having very different energetics, degrees of collimation, morphologies and ages are studied: OMC-1, Ceph A, DR 21, HH 211, HH 212 and S187IR.

By constructing a flux-velocity diagram for each outflow we found a common behavior for all of the outflows: each spectrum is flat at velocities lower than a break point followed by a power law, $dF/dv \propto v^{\gamma}$ with γ between -1.8 and -2.6, at higher velocities. Furthermore, a similar power

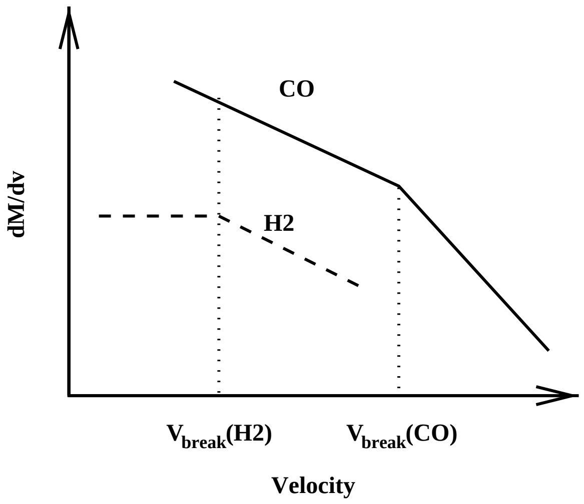

Fig. 3.— Schematic diagram of mass vs. velocity relation in CO and H_2 outflows.

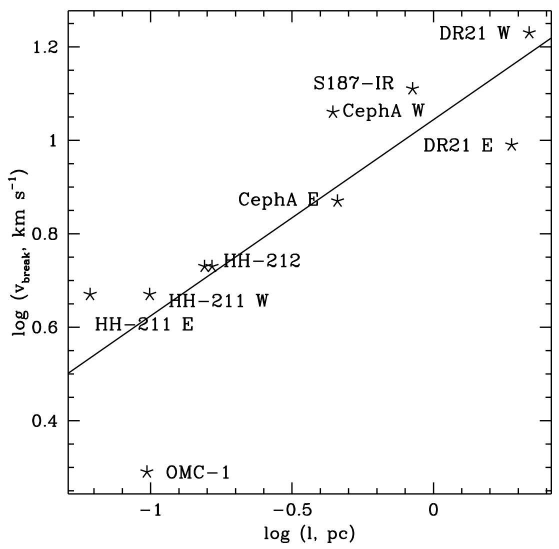

Fig. 4.— Correlation between break velocity and outflow length. The solid line corresponds to $v_{break} \propto l^{0.4}$.

law is found for solid angle and velocity.

Contrary to model predictions depending on the type of shocks involved, we found that the H_2 intensity is not a function of velocity. As a consequence, the flux-velocity spectrum implies a mass with velocity relation which is flat for low velocities and then decreases as a power law.

The velocity of the break between the flat and power law portions of the FV spectra occurs at low velocities (2 to 17 km s^{-1}) and is different for each outflow in our sample. Although the viewing angle could in principle produce a variety of break velocities and mass spectrum indexes, numerical simulations do not reproduce the observed relation between these three variables. Therefore, we favor age as the cause of the observed variations. CO outflows show a power law from low velocities up to a break point in the high velocity regime, beyond which the mass spectrum slope steepens. By comparing the H_2 and CO MV spectra, three velocity regimes are evident. The regime between $v_{break}(H_2)$ and $v_{break}(CO)$ show a similar power law for both molecules and may arise from shocked regions in the outflow where both molecules coexist. In this velocity region, evolutionary effects produce steeper slopes for older outflows, consistent with current models. The morphological similarities observed in H_2 and CO may arise in this velocity regime. In the regime below $v_{break}(H_2)$, H_2 also arises from shocked regions in the outflow and the excess CO emission may be produced by swept cool gas. At higher velocities, $v > v_{break}(CO)$, no H_2 emission is observed probably due to the dissociation of H_2.

A correlation between outflow length and γ or $v_{break}(H_2)$: $v_{break} \propto l^{0.4}$ and $\gamma \propto l^{0.08}$ is regarded as evidence of the effect of evolution of the outflow. As outflows age, it is argued that both γ and v_{break} increase and the reservoir of shocked H_2 gas produces a flat mass spectrum over a wide velocity range.

Recent numerical simulations by Downes & Cabrit (2001) show that the spectrum resulting for young outflows has a flat part for low velocities ($<$10-20 km s^{-1}) followed by a power law. Further work is needed in this direction, that would explain: 1) the evolutionary trends of the MV relation for both H_2 and CO outflows, 2) the observed intensity-velocity relation for H_2 emission and 3) the cause of the observed flatness and break in the H_2 spectrum.

Our results support a common physical origin for both CO and H_2 emission since they share similar properties, such as mass spectrum slope, bipolar outflow characteristics and low speeds. There is a strong association between the molecular outflows traced in each molecule and they are possibly produced in adjacent regions along the cooling zones behind turbulent shocks within molecular outflows.

Acknowledgments: We thank the OAN/SPM technical support staff and night assistants G. García, F. Montalvo, S. Monroy and G. Melgosa, for their valuable help during the observations. Our special thanks to Alex Raga for a careful revision of the manuscript and his valuable comments. Our appreciation to the referee, whose comments and suggestions greatly improved the final version. This work has been financed by grant 1N-120198 from DGAPA (UNAM).

REFERENCES

Cabrit, S., Raga, A., Gueth, F.: 1997, in IAU Symposium "Herbig-Haro Flows and the Birth of Low Mass Stars", eds. C. Bertout & B. Reipurth, p. 173.

Cruz-González, I., Carrasco, L., Ruiz, E., Salas, L., Skrutskie, M., Meyer, M., Sotelo, P., Barbosa, F., Gutiérrez, L., Iriarte, A., Cobos, F., Bernal, A., Sánchez, B., Valdéz, J., Argüelles, S., Conconi, P.: 1994, "CAMILA Infrared Camera/Spectrograph for OAN-SPM", in "Instrumentation in Astronomy VIII", eds. D.L. Crawford & E.R. Craine, Proc. SPIE 2198, p. 774.

Cruz-González, I, Salas, L., Porras, A.: 2001, RevMexAA, in preparation.

Davis, C. J., Berndsen, A., Smith, M. D., Chrysostomou, A., Hobson, J.: 2000, MNRAS, 314, 241.

Davis, C. J., Moriarty-Schieven, G., Eislöffel, J., Hoare, M. G., Ray, T. P., 1998, AJ, 115, 1118.

Downes, T. P., Cabrit, S.: 2001, in preparation.

Downes, T. P., Ray, T. P.: 1999, A&A, 345, 977.

Draine, B. T., Roberge, W. G., Dalgarno, A.: 1983, ApJ, 264, 485.

Fernandes, A. J. L., Brand, P. W. J. L., Burton, M. G.: 1997, MNRAS, 290, 216.

Hollenbach, D., McKee, C. F.: 1989, ApJ, 342, 306.

Kwan, J.: 1977, ApJ, 216, 713.

Lada, C. J., Fich, M.: 1996, ApJ, 459, 638.

Lee, C.-F., Stone, J., Ostriker, E., Mundy, L.: 2000, American Astronomical Society Meeting 196, #57.07.

Masson, C. R., Chernin, L. M.: 1992, ApJ, 387, L47.

Matzner, C. D., McKee, C. F.: 1999, ApJ, 526, L112.

Raga, A., Taylor, S. D., Cabrit, S., Biro, S.: 1995, A&A, 296, 833.

Richer, J. S., Shepherd, D. S., Cabrit, S., Bachiller, R., Churchwell, E.: 2000, in Protostars and Planets IV, Eds. B. Hannings, E. P. Boss & S. S. Russell, University of Arizona Press, Vol. 1, p. 867.

Rodríguez, L. F., Carral, P., Moran, J. M., Ho, P. T. P., 1982, ApJ, 260, 635.

Salas, L., Cruz-González, I., Porras, A.: 1998, ApJ, 500, 853.

Salas, L., Rosado, M., Cruz-González, I., Gutiérrez, L., Valdez, J., Bernal, A., Luna, E., Ruiz, E., Lazo, F.: 1999, ApJ, 511, 822.

Salas, L., Cruz-González, I., Rosado, M.: 2000, Rev. Mex. Astron.& Astrof., 36, 113.

Salas, L., Cruz-González, I., Rosado, M.: 2001, RevMexAA, submitted.

Salas, L., Hiriart, D., Cruz-González, I., Rozas, M.: 2001, RevMexAA, in preparation.

Shepherd, D. S., Watson, A. M., Sargent, A. I., Churchwell, E.: 1998, ApJ, 507, 861.

Smith, M. D., Suttner, G., Yorke, H. W.: 1997, A&A, 323, 223.

Stahler, S.: 1994, ApJ, 422, 616.

Suttner, G., Smith, M. D., Yorke, H. W., Zinnecker, H., 1997, A&A, 318, 595.

Wardle, M.: 1990, MNRAS, 246, 98.

Wilkin, F. P.: 1996, ApJ, 459, L31.

Yu, K.C.; Billawala, Y., Bally, J., 1999 AJ, 118, 2940.

Zhang, Q., Zheng, X.:1997, ApJ, 474, 719.